Cyanobacterial Growth on Municipal Wastewater Requires Low Temperatures

Travis C. Korosh[a,b], Andrew Dutcher[c], Brian F. Pfleger [a,d], and Katherine D. McMahon [c,e] *

[a] Department of Chemical and Biological Engineering, University of Wisconsin-Madison, Madison, WI 53706, United States
[b] Environmental Chemistry and Technology Program, University of Wisconsin-Madison, Madison, WI 53706, United States
[c] Department of Civil and Environmental Engineering, University of Wisconsin-Madison, Madison, WI 53706, United States
[d] Microbiology Doctoral Training Program, University of Wisconsin-Madison, Madison, WI 53706, United States
[e] Department of Bacteriology, University of Wisconsin-Madison, Madison, WI 53706, United States

* Corresponding author. 5552 Microbial Science Building, 1550 Linden Drive, Madison, WI 53706, United States. Phone: +1 608 890 2836. Fax: +1 608 262-9865. E-mail address: trina.mcmahon@wisc.edu.

Keywords: Nutrient removal, cyanobacteria, Synechococcus strain PCC 7002

ABSTRACT

Side-streams in wastewater treatment plants can serve as concentrated sources of nutrients (i.e. nitrogen and phosphorus) to support the growth of photosynthetic organisms that ultimately serve as feedstock for production of fuels and chemicals. However, other chemical characteristics of these streams may inhibit growth in unanticipated ways. Here, we evaluated the use of liquid recovered from municipal anaerobic digesters via gravity belt filtration as a nutrient source for growing the cyanobacterium *Synechococcus* sp. strain PCC 7002. The gravity belt filtrate (GBF) contained high levels of complex dissolved organic matter (DOM), which seemed to negatively influence cells. We investigated the impact of GBF on physiological parameters such as growth rate, membrane integrity, membrane composition, photosystem composition, and oxygen evolution from photosystem II. At 37°C, we observed an inverse correlation between GBF concentration and membrane integrity. Radical production was also detected upon exposure to GBF at 37°C. However, at 27°C the dose dependent relationship between GBF concentration and lack of membrane integrity was abolished. Immediate resuspension of strains in high doses of GBF showed markedly reduced oxygen evolution rates relative to the control. Together, this suggests that one mechanism responsible for GBF toxicity to *Synechococcus* is the interruption of photosynthetic electron flow and subsequent phenomena. We hypothesize this is likely due to the presence of a phenolic compounds within the DOM.

INTRODUCTION

The need to develop non-petroleum based platforms for fuel and chemical production is driving researchers to explore alternatives that harness renewable energy sources while minimizing other environmental impacts such as freshwater depletion, eutrophication, and the use of arable land for non-food production. Cyanobacteria are particularly attractive such platforms due to their genetic tractability, rapid growth rates, halotolerance, and ability to be grown on non-productive land with simple nutrient requirements (1, 2). According to published life cycle assessments, a large portion of the associated costs of culturing photoautotrophs are tied to upstream costs, such as CO_2 delivery and fertilizer application (3). High phosphorous/nitrogen removal rates and energy efficiencies have been reported for photobioreactor and open pond cultivation systems using wastewater streams rich in nitrogen and phosphorus (4, 5). Therefore, it may be possible to offset the requirement for fertilizer by reclaiming nutrients from wastewater. This approach could yield the sought-after non-petroleum based alternative while also providing a more effective means of nutrient and metal removal than conventional wastewater treatment (6–8). Side-streams from common wastewater treatment facilities such as supernatants or filtrates from solids-separation processes are particularly promising nutrient sources, assuming that cyanobacterial strains can efficiently use them.

Of the many streams available in common wastewater facilities, the liquid fraction of anaerobic digestate is thought to be the most attractive nutrient source (8–11). Although digestate is rich in the inorganic constituents necessary for growth, it also contains dissolved organic matter (DOM) that has been shown to limit photosynthetic activity (12). DOM is a heterogenous mixture of aliphatic and aromatic compounds derived from the decomposition of living organisms (13). The chemical nature of wastewater-derived DOM is largely governed by the type of treated waste and the treatment process, but it is largely comprised of hydrophilic, fulvic, and humic substances (14, 15). Humics can induce damaging permeability in model and bacterial membranes (16, 17). Various studies have also demonstrated that fulvic and humic acids can enhance the solubility of many organic compounds (18), which in turn would augment their bioavailability and potential toxicity. Many of these compounds are also photo-reactive, producing toxic hydrogen peroxide and hydroxyl radicals (19, 20), which is of significant concern for phototroph cultivation.

The mode of DOM toxicity is thought to involve interactions with the protein-pigment complex of photosystem II (PSII) in photosynthetic organisms, although the exact molecular mechanism remains unclear (21). When the rate of light induced damage to PSII exceeds its rate of repair, growth suppression and chlorosis result from the phenomena known as photoinhibition (22). When damage by photoinhibition is sufficient to hamper the natural ability to consume electrons generated by photosynthesis, reactive oxygen species (ROS) are concomitantly produced as an undesired by-product. Prolonged oxidative stress halts protein translation through oxidation of specific cysteine residues in the ribosomal elongation factors (23). Given these findings, it is increasingly evident that under conditions of sustained stress, regulation of electron flow is critical to maintain homeostasis in photosynthetic organisms (24, 25). Thus, it is important to understand the mechanisms by which DOM may be interrupting electron flow in order to capitalize on the potential of cyanobacteria to remediate wastewater and generate high-value chemicals.

In this study, we tested the practicality of using combined streams from a municipal wastewater plant as a nutrient source for cyanobacterial cultivation. We used the euryhaline cyanobacteria *Synechococcus* sp. strain PCC 7002 (PCC 7002) due to its exceptional tolerance to high-light intensity, salt, and other environmental stresses (26, 27). Initial attempts to grow PCC 7002 in this nutrient source under standard environmental conditions of 1% (v/v) CO_2, a temperature of 37°C, and illumination of 200 μmol photons $m^{-2}s^{-1}$ resulted in photobleached (white-yellow) cultures. In an effort to explain this observation while developing more feasible cultivation conditions, we assessed the effects of many environmental parameters during PCC 7002 cultivation in wastewater-based media by monitoring changes in growth rate, photopigment abundance, oxygen evolution rates, membrane integrity, and membrane composition. We observed a concentration and temperature dependent effect of GBF towards membrane and photosystem degradation. High GBF concentrations were associated with elevated DOM levels, and produced ROS in 37°C grown cultures. At 27°C, cultures adapted to growth on GBF had elevated levels of total fatty acids, high unsaturated fatty acid content, and elevated membrane integrity. Decreased photosynthetic oxygen production rates were noted upon exposure to high levels of GBF. This suggests bioavailability of the photoinhibitory compound in GBF is governed by changes in membrane content and composition that occur during growth at relatively high temperatures.

MATERIALS AND METHODS

Media and Growth Conditions

Synechococcus sp. strain PCC 7002 was obtained from the Pasteur Culture Collection of Cyanobacteria. Experiments were performed with a strain of PCC 7002 harboring a gentamicin resistance marker in the A2842 locus to maintain axenic cultures. Strains were grown and maintained on Medium A^+ (28) with 1.5% Bacto-Agar with gentamicin (30 μg/mL). Strains were cultured in 250 ml baffled flasks with 50 mL Medium A^+ with 5 μM $NiSO_4$ (29) with 1% CO_2-enriched air at 150 rpm in a Kuhner ISF1-X orbital shaker. Temperature was maintained at 37°C or 27°C and light intensity was fixed at approximately 200 μmol photons $m^{-2}s^{-1}$ or 100 μmol photons $m^{-2}s^{-1}$ via a custom LED panel. Strains were pre-acclimated to the culture conditions overnight before inoculating in fresh media. Optical density at 730 nm was measured in a Tecan M1000 plate reader.

Wastewater-derived media was obtained from the Nine Springs Wastewater Treatment Plant (Dane County, Wisconsin, USA). The plant is configured for biological nutrient removal via a modified University of Cape Town process with no internal nitrate recycling and stable performance yielding high secondary effluent quality (total phosphorus < 1 mg P/L, ammonia < 1 mg N/L, nitrate ~ 15 mg N/L) (30). Anaerobic digesters are used for solids stabilization and the resulting digested material is passed over a gravity belt filter for dewatering. The system includes an Ostara WASSTRIP process to recover phosphorus. This filtrate (GBF) served as the primary source of phosphorus and reduced nitrogen for our cultures, and effluent from the post-mainstream secondary treatment clarifier (secondary effluent) served as a diluent. GBF was filtered through a paper filter to remove any exceptionally large flocs, then stored at -80°C until use. Secondary effluent was collected one to four days before each experiment and held under refrigeration at approximately 2°C. Experimental media was comprised primarily of secondary clarifier effluent and GBF, combined in different proportions. Unless otherwise noted, GBF was used at a concentration of 12.5% (v/v) in secondary effluent. To meet complete nutrient requirements, the diluted GBF media was supplemented with trace metals and vitamin B12 at the concentrations found in Medium A^+, as well as KH_2PO_4 at a molar ratio of 1:32 soluble reactive phosphorus (SRP) to bioavailable nitrogen (the sum of NH_4^+ and NO_3^-). All media was buffered with Tris-HCl and adjusted to pH 8.0 with potassium hydroxide or hydrochloric acid before sterilization by autoclaving.

Staining, Flow Cytometry, and Fluorescence Measurements

The membrane integrity of cyanobacteria cells was recorded by a flow cytometer (FACSCalibur, BD Biosciences, San Jose, CA, USA). After growth in the respective media, cells were centrifuged (2 minutes, 5000 RCF), decanted, and resuspended in 1 mL of Tris-Buffered Saline (TBS) solution (pH 8.0). To identify membrane-compromised cells, SYTOX Green (Life Technologies) was also added to each sample (1 µM). SYTO 59 (Life Technologies) was added to each sample (1 µM) as a nucleic acid counterstain. As a control for a permeabilized membrane, cells were resuspended in 190 proof ethanol. SYTOX green fluorescence was visualized using 488 nm laser excitation and emission area was read using a 530/30 nm bandpass filter. The 633 nm laser coupled with a 661/16 bandpass filter was used for SYTO 59 visualization. Analysis of the cytometric data was carried out with CellQuest Pro (BDBiosciences, San Jose,CA, USA) software.

To assess reactive oxygen species production, cells (OD_{730} = 1) were incubated overnight in Medium A, GBF, GBF + 1 mM Dithiothreitol (DTT), GBF + 1 mM N-acetylcysteine (NAC), or Medium A + 100 µM methyl viologen as a positive control at 37°C with 5% CO_2 at a light intensity of 200 µmol photons $m^{-2}s^{-1}$. Cells were washed in TBS, and either Sytox Green (1 µM) or CellROX Orange reagent (Life Technologies) (5 µM) was added. After 30 min incubation in darkness at 37°C, fluorescence was measured (Ex/Em 545/565 nm for Cell ROX Orange) and (Ex/Em 504/523 nm for Sytox Green) in a Tecan M1000 plate reader.

GBF Characterization

SRP, ammonia, nitrate, and nitrite concentrations were determined for all secondary clarifier effluent and GBF samples used in these experiments. In addition, the GBF was tested for total suspended solids (TSS), volatile suspended solids (VSS) total solids (TS), and chemical oxygen demand (COD). Ammonia, SRP, and COD were determined by colorimetric tests using reagents from Hach. Nitrate and nitrite were determined using high performance liquid chromatography (Shimadzu) with a C18 column and photodiode array detector (31). TSS, VSS, and TS were measured according to Standard Method 2540 D, 2540 E, and 2540 B, respectively, with 47mm diameter glass fiber filters (Whatman) used for TSS and VSS (32). Fluorescence EEM measurements were conducted using a M1000 Tecan plate reader using a UV-transparent plate (Costar 3635). Fluorescence intensity was normalized to quinine sulfate units (QSU), where 1 QSU is the maximum fluorescence intensity of 1 ppm of quinine sulfate in 0.1 N H_2SO_4 at Ex/Em = 350/450. Rayleigh scatter effects were removed from the data set.

Biochemical analyses

Batch cultures were further assayed for dry cell weight (DCW), fatty acid content, oxygen evolution rates, and chlorophyll a content. Cells were concentrated by centrifugation, washed in TBS, and lyophilized overnight to obtain dry cell weights (DCW). Fatty acids from approximately 10 mg of DCW with 10 mg ml^{-1} pentadecanoic acid as an internal standard were converted to methyl-esters, extracted with n-hexane and analyzed by GC-FID on a Restek Stabilwax column (60m, 0.53 mm ID, 0.50 µm) (33). Photosynthetic oxygen evolution from whole cells was measured with a Unisense MicroOptode oxygen electrode with 10 mM $NaHCO_3$ illuminated with a slide projector at PPFD from 76-2700 µmol m^{-2} s^{-1} for 30 min at room temperature (34). Cells were collected by centrifugation and resuspended in the appropriate media to give an OD_{730} = 1.0. Chlorophyll a measurements were done via a 100% chilled methanol extraction procedure (35). Chlorophyll a was calculated via the following equation: $Chl_a = 16.29 * A^{665} - 8.54 * A^{652}$ (36).

RESULTS

GBF and secondary effluent characteristics

We measured nutrient concentrations from the batches of GBF collected over the 6 month experimental period (Table 1 and Table 2), to ascertain if it was a stable and reliable nutrient source for cultivating the cyanobacteria. Sampling points from the Nine Springs Wastewater Treatment Plant (Dane County, Wisconsin, USA) are shown in Figure 1. In order to calculate nutrient stoichiometries, we took the sum of NH_3-N and NO_3-N to be the bioavailable N. Nutrient levels in the GBF were markedly more variable than in the secondary effluent. The average molar ratio of bioavailable N to SRP was 35 ± 7 in GBF diluted with secondary effluent (12.5% v/v), as compared to 32 in Medium A^+.

We also measured DOM quality in the secondary effluent and GBF using excitation−emission matrix (EEM) fluorescence spectroscopy (37) because we hypothesized that DOM was linked to toxicity during cultivation. Secondary effluent contained diffuse constituents, including humic [excitation wavelengths (>280 nm) and emission wavelengths (>380 nm)] and fulvic acid-like [excitation wavelengths (<250 nm) and emission wavelengths (>350 nm)] spectra relative to Medium A^+ (Figure 2). The distinction between the two substances is historically based on solubility (38), but compositionally, fulvic acids contain more acidic functional groups than humic acids (39). The fulvic acid content in media preparations rose with increasing concentrations of GBF. Additionally, at high concentrations of GBF, a distinct region [excitation wavelengths (270 -290 nm) and emission wavelengths (340-400 nm)] was attributed to the presence of soluble microbial products, which include aromatic amino acids, carbohydrates, or phenols (37, 40). The exact composition of these products varies with plant configuration, but they are refractory to microbial degradation (41).

Exposure to GBF at high temperatures generates radicals

Preliminary growth experiments using GBF as a nutrient source were unsuccessful under standard cultivation conditions, due to cell photobleaching. We hypothesized that DOM in the media was in some way compromising membrane integrity, possibly via intracellular production of reactive oxygen species (ROS). Thus, we measured the ROS content and loss of membrane integrity in response to overnight GBF exposure at 37°C (Figure 3). We also examined the capacity of reducing agents Dithiothreitol (DTT) or N-acetylcysteine (NAC) to quench the media toxicity, since they have anti-oxidant properties due to the direct reduction of disulfide bonds or as precursors for the anti-oxidant glutathione (42). To measure their effect on the ROS production and culture viability after GBF exposure, we assessed ROS content and membrane integrity with either concurrent addition or preincubation of these quenching compounds in the diluted (12.5% v/v) GBF media. Addition of 100 μM methyl viologen to Medium A^+ served as a positive control. Exposure of cells to 12.5%-GBF media resulted in marked ROS production and membrane permeability, which no thiol treatment alleviated.

Dose-dependent toxicity of GBF is a function of growth temperature

To evaluate the effects of GBF dosage on PCC 7002 physiology, we measured growth rates in GBF concentrations ranging from 6.25%-12.5% (v/v) as a function of temperature (27°C vs 37°C) and light intensity (100 μmol m^{-2} s^{-1} vs 200 μmol m^{-2} s^{-1}) (Table 3). Medium A^+ served as a control. Higher temperatures depressed growth rates in GBF-based media. At 37°C, growth rates with 6.25% GBF at both 100 µmol m^{-2} s^{-1} and 200 µmol m^{-2} s^{-1} were most comparable to Medium A^{+}. Higher GBF concentrations had a more extreme effect on growth rates. However, this dose dependent effect of GBF on growth rate was abolished when the cultivation temperature was lowered to 27°C. At 200 µmol m^{-2} s^{-1} and 27°C, GBF cultures grew twice as slowly as the control and there was no significant difference between the tested GBF concentrations. Under 100 µmol m^{-2} s^{-1} and 27°C, growth rates were comparable across media conditions. Thus, successful cultivation using the more concentrated GBF media required adjusting both the light and temperature regimes.

Photobleaching is a common symptom of oxidative stress in photosynthetic organisms and is caused by the accumulation of ROS (43). To investigate the effects of GBF media on the photosynthetic pigmentation, we also performed whole cell absorbance scans at two different temperatures (27°C vs 37°C). Light intensity was held constant at 200 µmol m^{-2} s^{-1}. High GBF concentrations yielded enhanced chlorophyll, phycobilisome, and carotenoid degradation at 37°C (Figure 4a). At 27°C, photosynthetic pigments maintained intact relative to the control, regardless of GBF concentration, implying less ROS production at this temperature (Figure 4b).

We wondered whether the observed toxicity was imposed on cells early or late during the 72-hour cultivation period. To track the dynamics of GBF induced toxicity, we employed forward scatter flow cytometry using SYTO 59 as a counterstain to identify cells, which were subsequently visualized for membrane integrity using Sytox Green. Two distinct phases were identified upon exposure to GBF, which we interpreted as initial and chronic toxicity (Figure 4). Initial toxicity was defined as the change in Sytox Green positive events for samples analyzed during exponential growth, while chronic toxicity accounted for the change in Sytox Green events during linear growth. As was the case for 72-hour based growth rate, a relationship between both initial and chronic toxicity and increasing GBF concentrations was found at 37°C (Figure 5a). While we still detected considerable initial toxicity with GBF exposure at 27°C, there was less of an effect of dosage on chronic toxicity (Figure 5b). Altogether, this suggested that there was a temperature and cell-concentration dependent adaptation that ameliorated the susceptibility of cultures to GBF induced toxicity.

Exposure to GBF retards oxygen evolution

To better delineate the cause of initial toxicity associated with high GBF concentrations, we measured maximal oxygen evolution rates for strains briefly exposed to GBF media while increasing the light intensity. Measurements of photosynthetic oxygen evolution would allow for an indirect assessment of PSII activity and electron transfer. Cultures were grown to early linear phase in Medium A^+ or GBF media, washed, and resuspended in the appropriate media. Resuspension media was saturated with HCO_3^- (10 mM) in order to prevent inorganic carbon limitation. As expected, cells grown and assayed in Medium A^+ at 37°C showed a clear increase in O_2 evolution rate as the light intensity approached saturation at 2700 µmol m^{-2} s^{-1}, reaching a maximal rate of 240 ± 8 µmol O_2 (mg Chl a)$^{-1}$ h^{-1} (Figure 6a). Cells grown in Medium A^+ at 37°C but assayed in 12.5% GBF had diminished O_2 evolution rates at all light intensities, plateauing with a rate of 79 ± 6 µmol O_2 (mg Chl a)$^{-1}$ h^{-1} at an intensity of 270 µmol m^{-2} s^{-1} (Figure 6a). Thus, exposure to GBF under these conditions immediately caused a decrease in O_2 production.

Next, we examined the effect of temperature in a similar experiment. Assays carried out in Medium A^+ after growth in Medium A^+ at 27°C showed much higher maximal O_2 evolution rates at all tested light intensities than with cells grown at 37°C (Figure 6b), peaking at a rate 556 ± 102 µmol O_2 (mg Chl a)$^{-1}$ h^{-1}). This was expected because elevated O_2 evolution rates in low temperature grown cells have been previously reported and were attributed to a substantial change in photosystem stoichiometry (44). The O_2 evolution rates of cells grown in Medium A^+ at 27°C and then resuspended in 12.5% GBF stayed relatively constant at all of the tested intensities and were roughly 5-fold lower than in controls, with a maximal rate of 109 ± 22 μmol O_2 (mg Chl a)$^{-1}$ h^{-1} at an intensity of 75 μmol m^{-2} s^{-1}. We compared the above rates to those from cultures grown in 12.5% GBF at 27°C to test if adaptation to GBF was met with changes in photosynthetic activity. At tested light intensities, O_2 evolution rates with 27°C GBF-adapted cultures were not statistically different than with unadapted cultures. Finally, we conducted the inverse experiment, using cultures grown in GBF media at 27°C but assayed in Medium A^+ under saturating light. Interestingly, they displayed the highest evolution rate of any tested condition, at 944 ± 96 μmol O_2 (mg Chl a)$^{-1}$ h^{-1} (Figure 6b). This suggested that there is a period of dynamic photosynthetic adaptation to overcome the stress of GBF, and that when the stress is alleviated the cells have an enhanced capacity for photosynthetic activity.

Acclimation to GBF changes lipid content and composition

Based on the results described above, we hypothesized that the temperature dependent photosynthetic adaptation is related to changes in thylakoid membrane content and composition. We extracted total fatty acids of cultures grown at 27°C for 72 hours in 12.5% GBF or Medium A^+, and analyzed the content after derivatization. We could detect and resolve all major saturated and unsaturated fatty acid species (Table 4). Cultures grown in GBF had greater totals of assayed fatty acid species (27 ± 7 mg FAME gDCW^{-1}) when compared to cells grown in Medium A^+ (15 ± 1 mg FAME gDCW^{-1}) (Table 4). The most abundant fatty acid in all samples was 16:0 (42-45% of the total fatty acids). C18:2 Δ9,12 fatty acids comprised a significant fraction of Medium

A^+ grown cultures with 22% of the total fatty acid species. However, in GBF-grown cells the amount of C18:2 Δ9,12 fatty acids was only 15%, while C18:3 Δ9,12,15 fatty acids were twice as high in GBF grown cells (16%) than in Medium A^+ grown cells (9%) (Table 4). This suggests that cells were altering their membrane composition when grown in GBF, as compared to standard growth in Medium A^+.

DISCUSSION

The amount and distribution of arable land and potable water are projected to change over the next several decades due to climate change, while the rise in global population and standard of living are expected to increase demands (45). Integration of microalgal cultivation with industrial and municipal wastewater treatment circumvents many of the resource concerns raised over biofuel production (2), while simultaneously removing additional nutrients and pollutants present in the wastewater (46). However, under standard environmental conditions we were unable to obtain robust growth of PCC 7002 using a diluted municipal side stream as a nutrient source. We hypothesized that this effect may be due to the presence of DOM, which has been demonstrated to cause a decrease in photosynthetic performance in various strains of cyanobacteria (47–49). We investigated the effects of light intensity and temperature on the physiology of digestate grown cultures, in an effort to find conditions conducive to biomass generation and better understand the mechanisms of DOM toxicity.

We found that cultivation temperature was an important factor that allowed for the growth of PCC 7002 under high GBF concentrations. Numerous physiological processes are altered at low temperatures (50). Notably, the fatty acyl chains in the both the cytoplasmic and thylakoid membrane undergo a transition from a fluid to nonfluid state (51). The immediate cessation of oxygen evolution (Figure 6) and high rates of initial toxicity (Figure 5) upon GBF exposure with cells cultivated at tested temperatures suggests that the toxic compound rapidly crosses bacterial membranes. We propose that due to the decreased fluidity of the outer membrane at 27°C relative to 37°C, accessibility of humic and fulvic acids to the hydrophobic domains in the phospholipid bylayer is decreased, lessening the intracellular transport of the toxic compound(s) and initial and chronic toxicity.

Upon a shift to a lower temperature, cyanobacteria also alter the expression of desaturases to increase the unsaturated fatty acid content and maintain optimal membrane function (52). Optimal fluidity of thylakoid membranes is a critical factor in photosynthetic electron transport, due to the mobility of co-utilized redox components to both photosynthetic and respiratory complexes to ensure ideal electron flow (53, 54). It has been shown that temperature influences the kinetics governing the redox state of plastiquinone (PQ) through alterations in thylakoid membrane composition and fluidity (55). We believe that this temperature dependent alteration of the thylakoid membrane to circumvent GBF induced changes in the redox state is also an important component of the adaptive response, given the increase in unsaturated fatty acids observed during cultivation in GBF-based media (Table 4).

We propose that the herbicidal effect of GBF is partially due to the electron scavenging properties of phenolic moieties within in the DOM, given the symptoms of chlorophyll-bleaching as shown in Figure 3 and pronounced ROS production as evidenced by Figure 2 (56). These phenolic moieties are likely a component of the "soluble microbial products" found in our EEM scans (Figure 2). At low concentrations, phenolic photosynthetic electron transfer inhibitors such as 2,5-Dibromo-3-methyl-6-isopropyl-p-benzoquinone (DBMIB), alter the redox potential of the PQ pool of PSII by blocking forward electron transfer to the cytochrome b_6/f complex (57). DBMIB treatment has also been shown to substantially decrease inner mitochondrial membrane fluidity (58). This strong reduction of the PQ pool by DBMIB induces the phycobilisomes to physically move from PSII to PSI in a transition known as "state 2", thereby decreasing the ratio of reducing power to proton-motive force generated by photosynthesis (59). Marine *Synechococcus,* including PCC 7002, have also been shown to transition to state 2 upon shifts to lower temperature (60). Chronic exposure to phenolic herbicides eventually leads to radical-catalyzed back reactions that trigger the formation of ROS that facilitate complex destruction and cell death (43, 61–63). Some phenolic herbicides may also act as arylating agents, causing covalent binding to macromolecules via Michael addition and a depletion of thiol pools (64). The inability of the reducing agents we tested to maintain membrane integrity suggests that GBF-induced cytotoxicity is likely caused by redox cycling, and not arylation. Future efforts to increase tolerance to these toxicants might include disruption of the inhibitor binding sites (65, 66) or optimizing membrane fluidity (67).

CONCLUSIONS

Under standard cultivation conditions of 37°C with the cyanobacteria *Synechococcus* sp. strain PCC 7002, there was a dose-dependent relationship between liquid anaerobic digestate concentration and toxicity. This was met with ROS production and photopigment degradation. Digestate contained constituents of dissolved organic matter that were likely affecting photosynthetic electron transport. Decreasing the cultivation temperature to 27°C enabled robust cultivation at high digestate concentrations, resulting in high biomass productivities. This temperature dependent tolerance may be due to changes in membrane fluidity. Our study highlights the contributions of dissolved organic matter to photosynthetic growth and physiology in wastewater based media, as well as a potential mechanism for tolerance in low temperatures.

ACKNOWLEDGEMENTS

This work was funded by the US National Science Foundation (EFRI-1240268). TCK is the recipient of a National Institutes of Health (NIH) Biotechnology Training Fellowship (NIGMS-5 T32 GM08349) and a fellowship from the UW-Madison College of Engineering's Graduate Engineering Research Scholars (GERS) program. The authors are grateful to Richard Mikel, Matthew Dysthe, and Derek Jacobs for help with routine sampling.

REFERENCES

1. Oliver JWK, Atsumi S. 2014. Metabolic design for cyanobacterial chemical synthesis. Photosynth Res 120:249–61.
2. Pate R, Klise G, Wu B. 2011. Resource demand implications for US algae biofuels production scale-up. Appl Energy 88:3377–3388.
3. Clarens AF, Resurreccion EP, White M a, Colosi LM. 2010. Environmental life cycle comparison of algae to other bioenergy feedstocks. Environ Sci Technol 44:1813–9.
4. Posadas E, García-Encina PA, Domínguez A, Díaz I, Becares E, Blanco S, Muñoz R. 2014. Enclosed tubular and open algal-bacterial biofilm photobioreactors for carbon and nutrient removal from domestic wastewater. Ecol Eng 67:156–164.
5. Sturm BSM, Lamer SL. 2011. An energy evaluation of coupling nutrient removal from wastewater with algal biomass production. Appl Energy 88:3499–3506.
6. Hoffmann JP. 1998. Wastewater Treatment with Suspended and Nonsuspended Algae. J Phycol 34:757–763.
7. de la Noüe J, Laliberté G, Proulx D. 1992. Algae and waste water. J Appl Phycol 4:247–254.
8. Olguín EJ. 2012. Dual purpose microalgae–bacteria-based systems that treat wastewater and produce biodiesel and chemical products within a Biorefinery. Biotechnol Adv 30:1031–1046.
9. Wang L, Min M, Li Y, Chen P, Chen Y, Liu Y, Wang Y, Ruan R. 2010. Cultivation of green algae Chlorella sp. in different wastewaters from municipal wastewater treatment plant. Appl Biochem Biotechnol 162:1174–86.
10. Peccia J, Haznedaroglu B, Gutierrez J, Zimmerman JB. 2013. Nitrogen supply is an

important driver of sustainable microalgae biofuel production. Trends Biotechnol 31:134–8.

11. Rawat I, Ranjith Kumar R, Mutanda T, Bux F. 2011. Dual role of microalgae: Phycoremediation of domestic wastewater and biomass production for sustainable biofuels production. Appl Energy 88:3411–3424.
12. Pflugmacher S, Spangenberg M, Steinberg CEW. 1999. Dissolved organic matter (DOM) and effects on the aquatic macrophyte Ceratophyllum demersum in relation to photosynthesis, pigmentpattern and activity of detoxication enzymes. J Appl Bot 73:184–190.
13. Zsolnay Á. 2003. Dissolved organic matter: Artefacts, definitions, and functions, p. 187–209. *In* Geoderma.
14. Imai A, Fukushima T, Matsushige K, Kim Y-H, Choi K. 2002. Characterization of dissolved organic matter in effluents from wastewater treatment plants. Water Res 36:859–870.
15. Akhiar A, Torrijos M, Battimelli A, Carrère H. 2016. Comprehensive characterization of the liquid fraction of digestates from full-scale anaerobic co-digestion. Waste Manag.
16. Vigneault B, Percot A, Lafleur M, Campbell PGC. 2000. Permeability changes in model and phytoplankton membranes in the presence of aquatic humic substances. Environ Sci Technol 34:3907–3913.
17. Ojwang' LM, Cook RL. 2013. Environmental Conditions That Influence the Ability of Humic Acids to Induce Permeability in Model Biomembranes. Environ Sci Technol 47:8280–8287.
18. Chiou CT, Malcolm RL, Brinton TI, Kile DE. 1986. Water solubility enhancement of

some organic pollutants and pesticides by dissolved humic and fulvic acids. Environ Sci Technol;(United States) 20.

19. Zhang D, Yan S, Song W. 2014. Photochemically Induced Formation of Reactive Oxygen Species (ROS) from Effluents Organic Matter. Environ Sci Technol.

20. Lee E, Glover CM, Rosario-Ortiz FL. 2013. Photochemical formation of hydroxyl radical from effluent organic matter: Role of composition. Environ Sci Technol 47:12073–12080.

21. Laue P, Bährs H, Chakrabarti S, Steinberg CEW. 2014. Natural xenobiotics to prevent cyanobacterial and algal growth in freshwater: Contrasting efficacy of tannic acid, gallic acid, and gramine. Chemosphere 104:212–220.

22. Keren N, Krieger-Liszkay A. 2011. Photoinhibition: molecular mechanisms and physiological significance. Physiol Plant 142:1–5.

23. Nagano T, Kojima K, Hisabori T, Hayashi H, Morita EH, Kanamori T, Miyagi T, Ueda T, Nishiyama Y. 2012. Elongation factor G is a critical target during oxidative damage to the translation system of Escherichia coli. J Biol Chem 287:28697–704.

24. Foyer CH, Neukermans J, Queval G, Noctor G, Harbinson J. 2012. Photosynthetic control of electron transport and the regulation of gene expression. J Exp Bot 63:1637–61.

25. Voss I, Sunil B, Scheibe R, Raghavendra AS. 2013. Emerging concept for the role of photorespiration as an important part of abiotic stress response. Plant Biol (Stuttg) 15:713–22.

26. Ruffing AM. 2011. Engineered cyanobacteria: Teaching an old bug new tricks. bioe 2:136–149.

27. Xu Y, Alvey RM, Byrne PO, Graham JE, Shen G, Bryant DA. 2011. Expression of genes in cyanobacteria: adaptation of endogenous plasmids as platforms for high-level gene

expression in Synechococcus sp. PCC 7002. Methods Mol Biol 684:273–93.

28. Stevens SE, Patterson COP, Myers J. 1973. The Production of Hydrogen Peroxide by Blue-Green Algae: A Survey. J Phycol 9:427–430.

29. Sakamoto T, Bryant DA. 2001. Requirement of Nickel as an Essential Micronutrient for the Utilization of Urea in the Marine Cyanobacterium Synechococcus sp. PCC 7002. Microbes Environ 16:177–184.

30. Flowers JJ, Cadkin TA, McMahon KD. 2013. Seasonal bacterial community dynamics in a full-scale enhanced biological phosphorus removal plant. Water Res 47:7019–7031.

31. He S, McMahon KD. 2011. “Candidatus Accumulibacter” gene expression in response to dynamic EBPR conditions. ISME J 5:329–40.

32. Eaton AD, Franson MAH. 2005. Standard Methods for the Examination of Water & Wastewater, 21sted. American Public Health Association.

33. Lennen RM, Braden DJ, West RA, Dumesic JA, Pfleger BF. 2010. A process for microbial hydrocarbon synthesis: Overproduction of fatty acids in Escherichia coli and catalytic conversion to alkanes. Biotechnol Bioeng 106:193–202.

34. Sakamoto T, Bryant D a. 2002. Synergistic effect of high-light and low temperature on cell growth of the Delta12 fatty acid desaturase mutant in Synechococcus sp. PCC 7002. Photosynth Res 72:231–42.

35. Miyashita H, Adachi K, Kurano N, Ikemot H, Chihara M, Miyach S. 1997. Pigment composition of a novel oxygenic photosynthetic prokaryote containing chlorophyll d as the major chlorophyll. Plant cell Physiol 38:274–281.

36. Porra RJ, Thompson WA, Kriedemann PE. 1989. Determination of accurate extinction coefficients and simultaneous equations for assaying chlorophylls a and b extracted with

four different solvents: verification of the concentration of chlorophyll standards by atomic absorption spectroscopy. Biochim Biophys Acta (BBA)-Bioenergetics 975:384–394.

37. Chen W, Westerhoff P, Leenheer JA, Booksh K. 2003. Fluorescence Excitation-Emission Matrix Regional Integration to Quantify Spectra for Dissolved Organic Matter. Environ Sci Technol 37:5701–5710.

38. Lehmann J, Kleber M. 2015. The contentious nature of soil organic matter. Nature 1–9.

39. Peña-méndez ME, Havel J, Patočka J. 2005. Humic substances – compounds of still unknown structure□: applications in agriculture , industry , environment , and biomedicine. J Appl Biomed 3:13–24.

40. Cowgill RW. 1963. Fluorescence and the structure of proteins. I. Effects of substituents on the fluorescence of indole and phenol compounds. Arch Biochem Biophys 100:36–44.

41. Dignac MF, Ginestet P, Rybacki D, Bruchet A, Urbain V, Scribe P. 2000. Fate of wastewater organic pollution during activated sludge treatment: Nature of residual organic matter. Water Res 34:4185–4194.

42. Samuni Y, Goldstein S, Dean OM, Berk M. 2013. The chemistry and biological activities of N-acetylcysteine. Biochem Biophys 1830:4117–4129.

43. Latifi A, Ruiz M, Zhang C-C. 2009. Oxidative stress in cyanobacteria. FEMS Microbiol Rev 33:258–78.

44. Sakamoto T, Bryant D a. 1998. Growth at low temperature causes nitrogen limitation in the cyanobacterium Synechococcus sp. PCC 7002. Arch Microbiol 169:10–9.

45. Parry ML, Rosenzweig C, Iglesias A, Livermore M, Fischer G. 2004. Effects of climate change on global food production under SRES emissions and socio-economic scenarios.

Glob Environ Chang 14:53–67.

46. Wang Y, Ho SH, Cheng CL, Guo WQ, Nagarajan D, Ren NQ, Lee DJ, Chang JS. 2016. Perspectives on the feasibility of using microalgae for industrial wastewater treatment. Bioresour Technol 222:485–497.

47. Sun B, Tanji Y, Unno H. 2006. Extinction of cells of cyanobacterium Anabaena circinalis in the presence of humic acid under illumination. Appl Microbiol Biotechnol 72:823–828.

48. Shao J, Wu Z, Yu G, Peng X, Li R. 2009. Allelopathic mechanism of pyrogallol to Microcystis aeruginosa PCC7806 (Cyanobacteria): From views of gene expression and antioxidant system. Chemosphere 75:924–928.

49. Gjessing ET, Alberts J., Bruchet A, Egeberg PK, Lydersen E, McGown LB, Mobed JJ, Münster U, Pempkowiak J, Perdue M, Ratnawerra H, Rybacki D, Takacs M, Abbt-Braun G. 1998. Multi-method characterisation of natural organic matter isolated from water: characterisation of reverse osmosis-isolates from water of two semi-identical dystrophic lakes basins in Norway. Water Res 32:3108–3124.

50. Morgan-Kiss RM, Priscu JC, Pocock T, Gudynaite-Savitch L, Huner NPA. 2006. Adaptation and Acclimation of Photosynthetic Microorganisms to Permanently Cold Environments. Microbiol Mol Biol Rev 70:222–252.

51. De Mendoza D. 2014. Temperature Sensing by Membranes. Annu Rev Microbiol 68:101–16.

52. Singh SC, Sinha RP, Häder D. 2002. Role of Lipids and Fatty Acids in Stress Tolerance in Cyanobacteria. Acta Protozool 41:297–308.

53. Mullineaux CW. 2014. Electron transport and light-harvesting switches in cyanobacteria. Front Plant Sci 5:1–6.

54. Liu L-N. 2015. Distribution and dynamics of electron transport complexes in cyanobacterial thylakoid membranes. Biochim Biophys Acta - Bioenerg.

55. Klementiev KE, Tsoraev G V, Tyutyaev E V, Zorina AA, Feduraev P V, Allakhverdiev SI, Paschenko VZ. 2017. Membrane fluidity controls redox-regulated cold stress responses in cyanobacteria. Photosynth Res 0:0.

56. Pallett KE, Dodge AD. 1980. Studies into the Action of Some Photosynthetic Inhibitor Herbicides. J Exp Bot 31:1051–1066.

57. Schoepp B, Brugna M, Riedel A, Nitschke W, Kramer DM. 1999. The Qo-site inhibitor DBMIB favours the proximal position of the chloroplast Rieske protein and induces a pK-shift of the redox-linked proton. FEBS Lett 450:245–250.

58. Siedow JN, Huber SC, Moreland DE. 1979. Effects of dibromothymoquinone on mung bean mitochondrial electron transfer and membrane fluidity. BBA - Bioenerg 547:282–295.

59. Mao H Bin, Li GF, Ruan X, Wu QY, Gong YD, Zhang XF, Zhao NM. 2002. The redox state of plastoquinone pool regulates state transitions via cytochrome b6f complex in Synechocystis sp. PCC 6803. FEBS Lett 519:82–86.

60. Mackey KRM, Paytan A, Caldeira K, Grossman AR, Moran D, McIlvin M, Saito MA. 2013. Effect of temperature on photosynthesis and growth in marine Synechococcus spp. Plant Physiol 163:815–29.

61. Krieger-Liszkay A, Fufezan C, Trebst A. 2008. Singlet oxygen production in photosystem II and related protection mechanism. Photosynth Res 98:551–564.

62. Idedan I, Tomo T, Noguchi T. 2011. Herbicide effect on the photodamage process of photosystem II: Fourier transform infrared study. Biochim Biophys Acta - Bioenerg

1807:1214–1220.

63. Nishiyama Y, Allakhverdiev SI, Murata N. 2011. Protein synthesis is the primary target of reactive oxygen species in the photoinhibition of photosystem II. Physiol Plant 142:35–46.

64. Wang X, Thomas B, Sachdeva R, Arterburn L, Frye L, Hatcher PG, Cornwell DG, Ma J. 2006. Mechanism of arylating quinone toxicity involving Michael adduct formation and induction of endoplasmic reticulum stress. Proc Natl Acad Sci U S A 103:3604–9.

65. Ajlani G, Kirilovsky D, Picaud M, Astier C. 1989. Molecular analysis of psbA mutations responsible for various herbicide resistance phenotypes in Synechocystis 6714. Plant Mol Biol 13:469–79.

66. Lee TX, Metzger SU, Cho YS, Whitmarsh J, Kallas T. 2001. Modification of inhibitor binding sites in the cytochrome bf complex by directed mutagenesis of cytochrome b6 in Synechococcus sp. PCC 7002. Biochim Biophys Acta - Bioenerg 1504:235–247.

67. Gombos Z, Wada H, Murata N. 1994. The recovery of photosynthesis from low-temperature photoinhibition is accelerated by the unsaturation of membrane lipids: a mechanism of chilling tolerance. Proc Natl Acad Sci U S A 91:8787–91.

FIGURE LEGENDS

Figure 1. Flow diagram and nutrient streams obtained from the Nine Springs Wastewater Treatment Plant (Dane County, Wisconsin, USA). Stars indicate sampling points.

Figure 2. Excitation Emission Matrix of wastewater medias. Fluorescence values were normalized to 1 ppm of quinine sulfate in 0.1 N H_2SO_4 at Ex/Em = 350/450 nm.

Figure 3. Reactive oxygen species and membrane integrity assay. Cells were grown to early linear phase in Medium A^+ or 12.5% GBF with the appropriate treatment under continuous illumination (200 µE m^{-2} s^{-1}) with 1 % CO_2 at 37°C. Fluorescence values were normalized to $OD_{730.}$ The values represent the mean ± SD of biological triplicates.

Figure 4. Absorption spectra of GBF exposed strains as a function of temperature. Cultures were grown in Medium A^+, 6.25 %, or 12.5 % (v/v) GBF media under continuous illumination (200 µE m^{-2} s^{-1}) with 1 % CO_2 at 37°C (A) or 27°C (B) for 72 hours. The spectra were recorded in dilute cell suspensions and normalized to an OD_{730}. The peak at 637 nm is due to phycobilisomes, the peak at 683 nm is due to chlorophyll a, and the peak at 438 nm is due to carotenoids.

Figure 5. Initial and chronic toxicity of cultures grown in Medium A^+, 6.25 %, 9.9 %, or 12.5 % (v/v) GBF media under continuous illumination (200 µE m^{-2} s^{-1}) with 1 % CO_2 at 37°C (A) or

27°C (B) for 72 hours. Initial toxicity was defined as the change in Sytox Green positive events for samples analyzed during exponential growth. Chronic toxicity accounted for the change in Sytox Green events during linear growth. A measure of < 0 chronic toxicity means that the samples recovered following a period of initial toxicity.

Figure 6. Rates of oxygen evolution as a function of acclimation temperature and light intensity. Cells were grown to early linear phase in Medium A^+ or 12.5% GBF under continuous illumination (200 µE m^{-2} s^{-1}) with 1 % CO_2 at 37°C (A) or 27°C (B). Cells were pelleted, resuspended in Medium A^+ or 12.5% GBF, and the rate of maximal oxygen evolution was measured with 10 mM HCO_3^- as an electron acceptor at increasing light intensities. The values represent the mean ± SE of biological duplicates.

TABLES

Table 1. Nutrient composition of batch of 100% GBF used for subsequent experiments

Analyte	Concentration[a] (mg L^{-1}) (±SD)
NH_3–N	1180 ± 135
NO_3–N	7.5 ± 0.04
SRP	78 ± 10
COD	735 ± 4
TSS	467 ± 123
VSS	18 ± 2
TS	2350 ± 36
TS (Glass Fiber Filtered)	2030 ± 42
TS (0.45 um membrane filtered)	2000 ± 151

[a]Values shown represent the mean ± standard deviation (SD) of at least three technical replicates.

Table 2. Characteristics of GBF and secondary effluent over the 6 month experimental period.

Source	Analyte	Concentration[a] (mg L^{-1}) (±COV)
GBF	NH_3–N	920 ± 22%
	NO_3–N	3.9 ± 43%
	SRP	54 ± 27%
Secondary Effluent	NH_3–N	n.d.
	NO_3–N	19.3 ± 6.6%
	SRP	n.d.

[a]Values shown represent the mean ± coefficient of variation (COV) of at least three technical replicates.

Table 3. Growth Rates with varying Temperature and Light Intensity

Media	**Light Intensity ($\mu E\ m^{-2}\ s^{-1}$)**	**Temperature (°C)**	**Growth Rate (±SD) (OD day^{-1})**
A^+	200	37	0.66 ± 0.04
6.25% GBF	200	37	0.58 ± 0.05
12.5% GBF	200	37	0.05 ± 0.01
A^+	100	37	0.28 ± 0.01
6.25% GBF	100	37	0.24 ± 0.01
9.9% GBF	100	37	0.11 ± 0.02
12.5% GBF	100	37	0.02 ± 0.00
A^+	200	27	0.73 ± 0.08
6.25% GBF	200	27	0.32 ± 0.03
9.9% GBF	200	27	0.42 ± 0.06
12.5% GBF	200	27	0.28 ± 0.04
A^+	100	27	0.25 ± 0.01
6.25% GBF	100	27	0.26 ± 0.02
9.9% GBF	100	27	0.24 ± 0.01
12.5% GBF	100	27	0.26 ± 0.02

[a] Linear growth rates of cultures grown in Medium A^+ or GBF with the appropriate treatment under continuous illumination (200 $\mu E\ m^{-2}\ s^{-1}$ or 100 $\mu E\ m^{-2}\ s^{-1}$) with 1 % CO_2 at 37°C or 27°C. The values represent the mean ± SD of biological triplicates.

Table 4. Fatty acid content and composition of cultures grown in Medium A$^+$ or 12.5% GBF media under continuous illumination (200 μE m^{-2} s^{-1}) at 27°C for 72 hours

Growth Conditions[1]		Fatty Acids Species					
		C16:0	**C16:1 Δ9**	**C18:0**	**C18:1 Δ9**	**C18:2 Δ9,12**	**C18:3 Δ9,12,1**
Medium A$^+$	mg FA gDCW^{-1}	6.7 ± 0.7	2.0 ± 0.1	0.2 ± 0.1	1.5 ± 0.2	3.3 ± 0.2	1.4 ± 0.
	% FA	44 ± 1	13 ± 1	2 ± 0	10 ± 0	22 ± 1	9 ± 1
GBF	mg FA gDCW^{-1}	11.6 ± 3.1	3.5 ± 0.8	1.3 ± 0.3	2.2 ± 0.7	3.9 ± 0.8	4.4 ± 1.
	% FA	43 ± 0	13 ± 0	5 ± 0	8 ± 0	15 ± 1	16 ± 1

[1] Strains were grown in the Medium A$^+$ or 12.5% GBF media under continuous illumination (200 μE m^{-2} s^{-1}) at 27°C for 72 hours. Fatty acids were extracted and derivatized as previously described. The values represent the mean ± SD of two independent experiments.

FIGURES

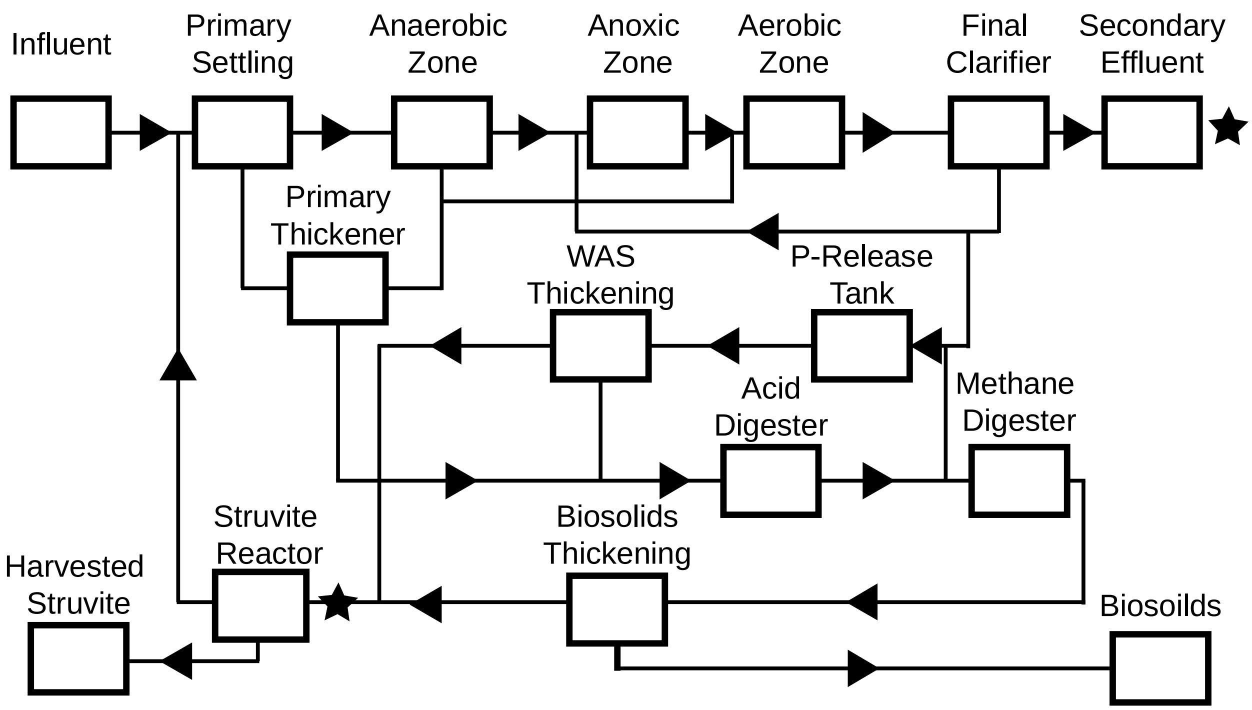

5

Figure 1. Flow diagram and nutrient streams obtained from the Nine Springs Wastewater Treatment Plant (Dane County, Wisconsin, USA). Stars indicate sampling points.

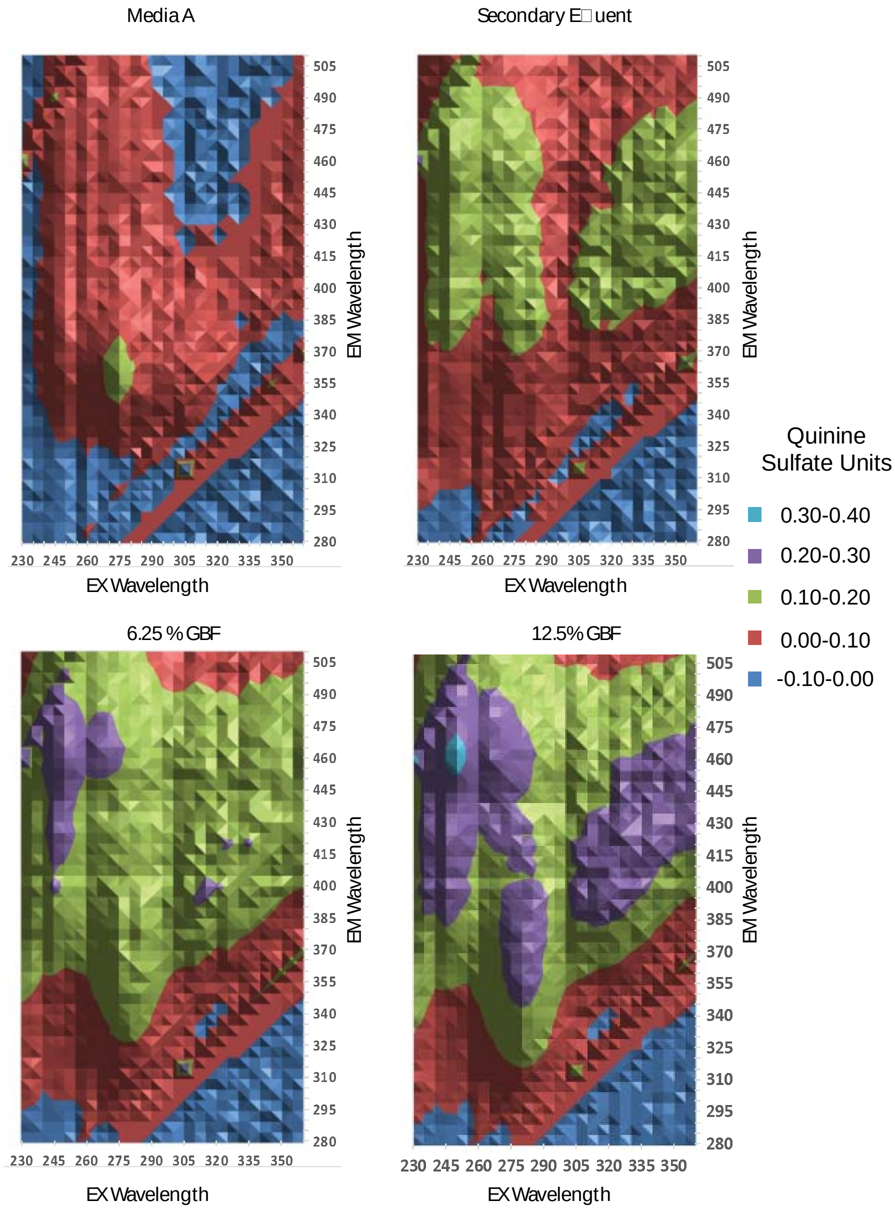

Figure 2. Excitation Emission Matrix of wastewater medias. Fluorescence values were normalized to 1 ppm of quinine sulfate in 0.1 N H_2SO_4 at Ex/Em = 350/450 nm.

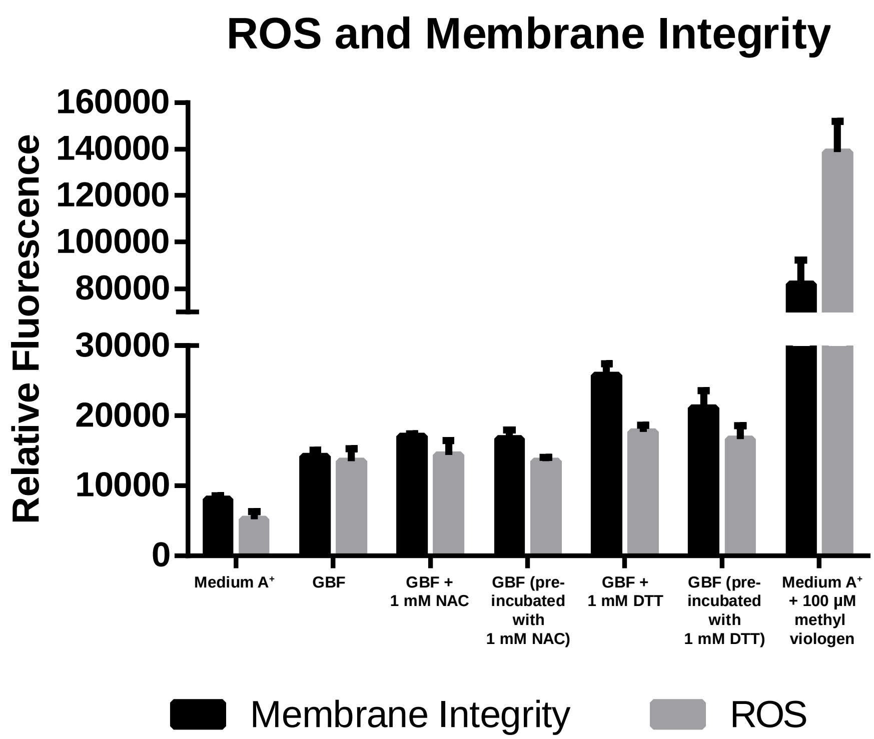

Figure 3. Reactive oxygen species and membrane integrity assay. Cells were grown to early linear phase in Medium A$^+$ or 12.5% GBF with the appropriate treatment under continuous illumination (200 µE m^{-2} s^{-1}) with 1 % CO_2 at 37°C. Fluorescence values were normalized to OD_{730}. The values represent the mean ± SD of biological triplicates.

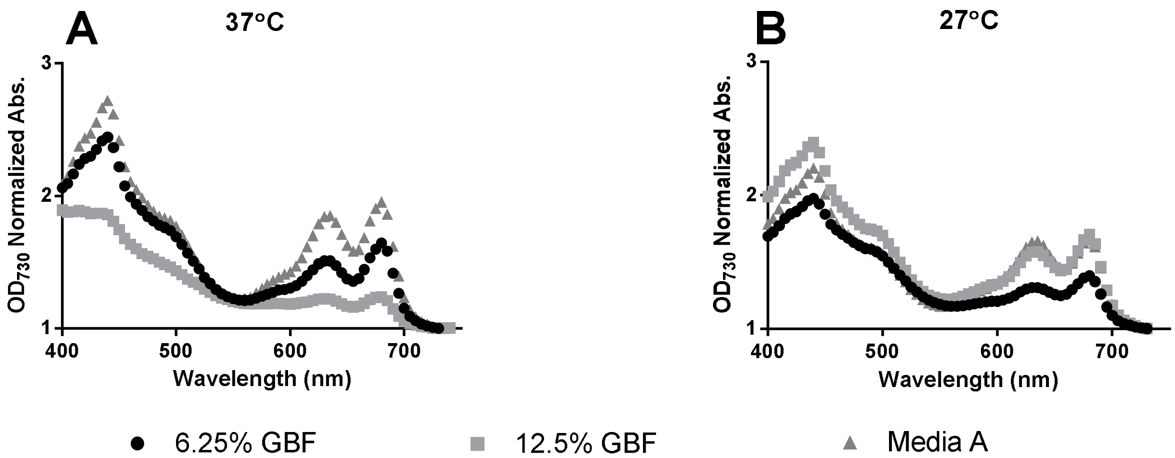

Figure 4. Absorption spectra of GBF exposed strains as a function of temperature. Cultures were grown in Medium A$^+$, 6.25 %, or 12.5 % (v/v) GBF media under continuous illumination (200 µE m^{-2} s^{-1}) with 1 % CO_2 at 37°C (A) or 27°C (B) for 72 hours. The spectra were recorded in dilute cell suspensions and normalized to an OD_{730}. The peak at 637 nm is due to phycobilisomes, the peak at 683 nm is due to chlorophyll a, and the peak at 438 nm is due to carotenoids.

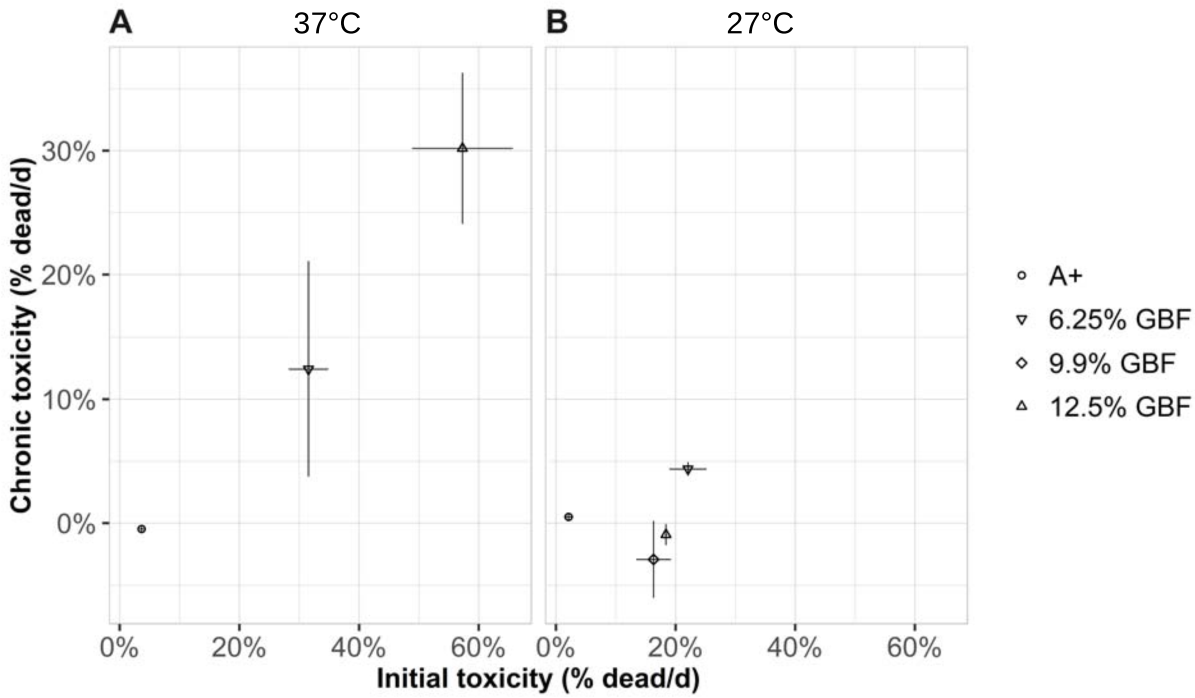

Figure 5. Initial and chronic toxicity of cultures grown in Medium A^{+}, 6.25 %, 9.9 %, or 12.5 % (v/v) GBF media under continuous illumination (200 µE m^{-2} s^{-1}) with 1 % CO_2 at 37°C (A) or 27°C (B) for 72 hours. Initial toxicity was defined as the change in Sytox Green positive events for samples analyzed during exponential growth. Chronic toxicity accounted for the change in Sytox Green events during linear growth. A measure of < 0 chronic toxicity means that the samples recovered following a period of initial toxicity.

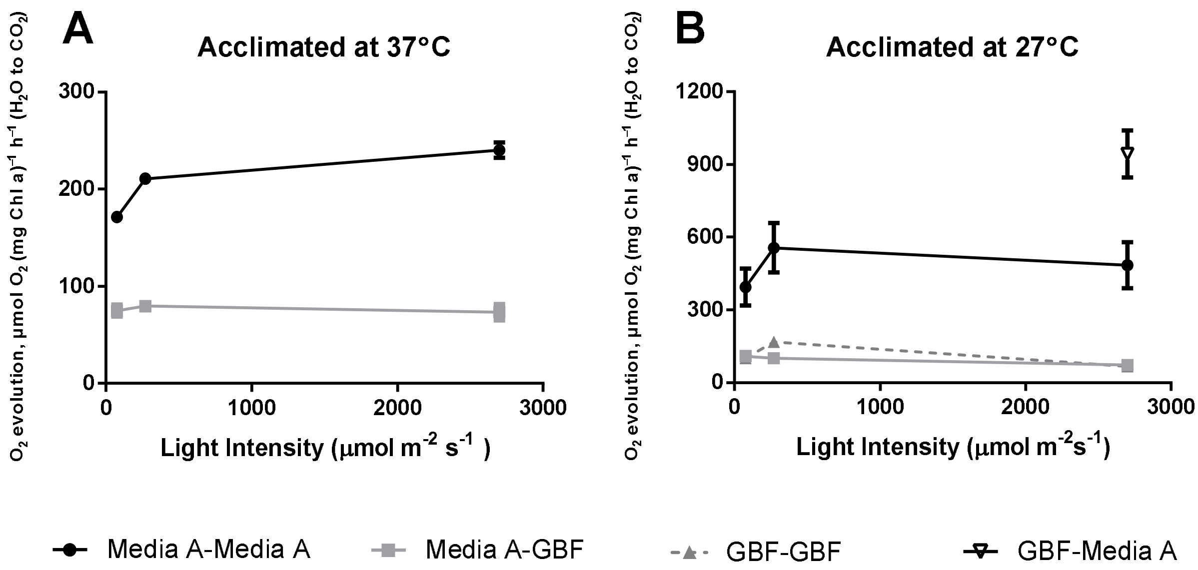

Figure 6. Rates of oxygen evolution as a function of acclimation temperature and light intensity. Cells were grown to early linear phase in Medium A^+ or 12.5% GBF under continuous illumination (200 μE m^{-2} s^{-1}) with 1 % CO_2 at 37°C (A) or 27°C (B). Cells were pelleted, resuspended in Medium A^+ or 12.5% GBF, and the rate of maximal oxygen evolution was measured with 10 mM HCO_3^- as an electron acceptor at increasing light intensities. The values represent the mean ± SE of biological duplicates.